Geochemistry Geophysics Geosystems G3

Article
Volume 13, Number 2
29 February 2012
Q02012, doi:10.1029/2011GC003920
ISSN: 1525-2027

Published by AGU and the Geochemical Society

Total CO_2 output from Vulcano island (Aeolian Islands, Italy)

Salvatore Inguaggiato
Istituto Nazionale di Geofisica e Vulcanologia, Sezione di Palermo, via Ugo La Malfa 143, I-90145 Palermo, Italy (s.inguaggiato@pa.ingv.it)

Agnes Mazot
GNS Science Wairakei Research Centre, 114 Karetoto Road, Wairakei, Private Bag 2000, Taupo 3352, New Zealand

Iole Serena Diliberto
Istituto Nazionale di Geofisica e Vulcanologia, Sezione di Palermo, via Ugo La Malfa 143, I-90145 Palermo, Italy

Claudio Inguaggiato
Facoltà di Scienze Geologiche, Università di Palermo, I-90133 Palermo, Italy

Paolo Madonia, Dmitri Rouwet, and Fabio Vita
Istituto Nazionale di Geofisica e Vulcanologia, Sezione di Palermo, via Ugo La Malfa 143, I-90145 Palermo, Italy

[1] Total CO_2 output from fumaroles, soil gas, bubbling gas discharges and water dissolved gases discharged from the island, was estimated for Vulcano island, Italy. The CO_2 emission from fumaroles from the La Fossa summit crater was estimated from the SO_2 crater output, while CO_2 discharged through diffuse soil emission was quantified on the basis of 730 measurements of CO_2 fluxes from the soil of the island, performed by using the accumulation chamber method. The results indicate an overall output of $\cong$500 t day^{-1} of CO_2 from the island. The main contribution to the total CO_2 output comes from the summit area of the La Fossa cone (453 t day^{-1}), with 362 t day^{-1} from crater fumaroles and 91 t day^{-1} from crater soil degassing. The release of CO_2 from peripheral areas is $\cong$20 t day^{-1} by soil degassing (Palizzi and Istmo areas mainly), an amount comparable to both the contribution of water dissolved CO_2 (6 t day^{-1}), as well as to seawater bubbling CO_2 (4 t day^{-1} measured in the Istmo area). Presented data (September 2007) refer to a period of moderate solphataric activity, when the fumaroles temperature were 450°C and gas/water molar ratio of fumaroles was up to 0.16. The calculated total CO_2 emission allows the estimation of the mass release and related thermal energy from the volcanic-hydrothermal system.

Components: 9200 words, 15 figures, 8 tables.

Keywords: CO_2 flux; CO_2 output; SO_2 flux; Vulcano island.

Index Terms: 8410 Volcanology: Geochemical modeling (1009, 3610); 8424 Volcanology: Hydrothermal systems (0450, 1034, 3017, 3616, 4832, 8135); 8430 Volcanology: Volcanic gases.

Received 17 October 2011; **Revised** 10 January 2012; **Accepted** 19 January 2012; **Published** 29 February 2012.

Inguaggiato, S., A. Mazot, I. S. Diliberto, C. Inguaggiato, P. Madonia, D. Rouwet, and F. Vita (2012), Total CO_2 output from Vulcano island (Aeolian Islands, Italy), *Geochem. Geophys. Geosyst.*, *13*, Q02012, doi:10.1029/2011GC003920.

1. Introduction

[2] Vulcano island, the southernmost island of the Aeolian Archipelago (Figure 1), is an active volcano that has been in state of solphataric activity since the last eruption (1888–1890). In 2007, the main exhalative activity is located in the northern part of the island (Figure 1) and is characterized by the presence of (1) a wide fumarolic field, on the active part of the edifice of "La Fossa" crater, (100°C < T < 450°C); (2) low temperature fumaroles (T < 100°C) and seawater bubbling gases in the Baia Levante area; and (3) strong soil degassing occurring in the Vulcano Porto area and around the volcanic edifice, where the active tectonic discontinuities drive CO_2 to the surface [*Capasso et al.*, 1997; *Diliberto et al.*, 2002]. Finally, numerous carbon-rich thermal wells (up to 80°C) in the Vulcano Porto area, testify the presence of a geothermal system with equilibrium temperature around 200°C [*Federico et al.*, 2010].

[3] During the last decades Vulcano island showed an indication of renewed activity, highlighted by the increase of temperatures and volatile fluxes from the fumarolic area and by strong compositional variations in the output of crater fumaroles, as well as in thermal waters. The most intensive variations have been interpreted as due to increase of magmatic component in the fluid release, with respect to hydrothermal one [*Chiodini et al.*, 1996; *Capasso et al.*, 1997; *Capasso and Inguaggiato*, 1998; *Paonita et al.*, 2002; *Diliberto*, 2011].

[4] A decrease in pressure caused by rock fracturation or rising of a magma batch toward the surface determines an overpressure of volatiles in the magma, consequently followed by their exsolution. These volatiles interact with shallow aquifers and also feed soil degassing as well as fumarolic activity [*Taran et al.*, 1986; *Capasso et al.*, 1997; *Nuccio and Paonita*, 2001; *Inguaggiato et al.*, 2000, 2011]. At Vulcano island, isotopic and compositional data of volatiles discharged from volcanic systems confirm the contribution of a magmatic source.

[5] Generally, carbon dioxide represents the main constituent of anhydrous gases discharged from the summit areas of volcanoes through plumes or crater fumaroles [*Chiodini et al.*, 2005]. This parameter was considered to study the volatile outputs in many volcanic systems [*Chiodini et al.*, 1996; *Favara et al.*, 2001; *Cardellini et al.*, 2003; *Chiodini et al.*, 2005; *Inguaggiato et al.*, 2005; *Pecoraino et al.*, 2005; *Mazot et al.*, 2011] and in geochemical monitoring programs aiming to highlight changes in the volcanic activity [*Brusca et al.*, 2004; *Carapezza et al.*, 2004; *Werner and Cardellini*, 2006; *Inguaggiato et al.*, 2011].

[6] Many geochemical investigations on volcanic systems focused so far on the study of extensive parameters (like mass flows of H_2O, SO_2 or CO_2) as tools to quantify the mass involved in the degassing processes both during active and quiescent phases [*Allard et al.*, 1994; *Italiano et al.*, 1998; *Aiuppa et al.*, 2005, 2010; *Allard et al.*, 2005, *Inguaggiato et al.*, 2011]. The goals of the present work are the estimation of the CO_2 output of discharged fluids from Vulcano island, on the basis of the emitted CO_2 in all the carbon species (CO_2gas, CO_2dissolved, HCO_3), and the realization of a soil CO_2-degassing map, which is useful to identify anomalous degassing areas and suitable sites for installation of new geochemical monitoring systems to evaluate the level of volcanic activity. To reach this aim, a geochemical survey to measure the soil CO_2 fluxes was performed in September 2007 covering the whole surface of Vulcano island. Particular attention was paid to the summit of the active cone and to Levante beach, which are the areas subjected to the most intense exhaling activity. In order to obtain a complete picture of carbon output, fumarolic gases and thermal well waters were also sampled and analyzed.

2. State of the Art

[7] The evaluation of output of CO_2 degassed from volcanic systems has a relevance both for geochemical monitoring activities, as well as for the evaluation of magmatic-CO_2 contribution to the global carbon cycle. The volcanic activity represents the main natural contributor of CO_2 emitted into the atmosphere [*Brantley and Koepenick*, 1995; *Arthur*, 2000; *Mörner and Etiope*, 2002]. For this reason, any work focused to estimate the CO_2 degassing from a volcanic system represents a contribution to refine previous global estimations and to achieve a more realistic value of the total global output of volcanic CO_2.

[8] A great amount of soil, fumaroles and plume CO_2 fluxes were measured during quiescent activity (inter-eruptive periods) of active volcanoes [*Carbonnelle et al.*, 1985; *Baubron et al.*, 1990; *Baubron et al.*, 1991; *Aiuppa et al.*, 2010; *Inguaggiato et al.*, 2011]. Changes in the CO_2 fluxes have so far been correlated with other variations registered by the parameters related to the volcanic activity like major explosion (paroxysms),

Figure 1. Satellite view of Vulcano island (Aeolian Archipelago, Sicily Italy). The main areas of shallow fluid investigated are indicated: Thermal wells area (located around Vulcano village), Craters fumaroles and Beach fumaroles areas.

increase of the frequency of explosive activity and/or onset of effusive activity [*Carapezza et al.*, 2004; *Brusca et al.*, 2004; *Aiuppa et al.*, 2010; *Inguaggiato et al.*, 2011].

[9] At Vulcano island, carbon dioxide emissions are characterized and estimated in various studies. In particular, *Baubron et al.* [1991] and *Chiodini et al.* [1996] estimated the CO_2 emitted from the summit area of the active cone, while *Diliberto et al.* [2002] presented time variations of diffuse degassing from the base of the active cone, also highlighting the time relationships between changes in CO_2 diffuse flux from a peripheral area and volcanic activity expressed through the fumaroles release from the summit area of the active cone.

[10] The estimation of diffuse soil degassing in the Porto area (northeast side of Vulcano) has been carried out since 1984 [*Baubron et al.*, 1990; *Badalamenti et al.*, 1988, 1991]. Former estimations showed a wide range of values, especially in the 1984–1988 period when a range between 70 and 1,000 t day^{-1} was estimated on the basis of 55 measurement points covering an area of 2.2 km^2. In 1993, a flux of 75 t day^{-1} was reported from the same area utilizing 420 points of measurement performed with the accumulation chamber method [*Chiodini et al.*, 1996, 1998].

[11] From the summit area diffuse soil degassing was estimated to be 115 t day^{-1} in 1990 (150 measurement points [*Baubron et al.*, 1991]) and 200 t day^{-1} in 1995 (91 measurement points [*Chiodini et al.*, 1996]), respectively. In 1990, the carbon dioxide discharged from the fumaroles of the Istmo area was estimated to be around 6.5 t day^{-1} [*Italiano and Nuccio*, 1994].

[12] Vulcano island has also been studied in order to characterize the chemical composition of the volcanic plume. Despite the fact that Vulcano island does not show a real plume, like an open conduct degassing volcano, but only a summit degassing fumarolic field with outlet temperature up to 450°C, this area has been used as a natural laboratory to test new remote sensing techniques and different prototypes. In particular, *Mori et al.* [1995] used a FT-IR Spectral Radiometer for remote measurements on the Vulcano's plume; *Aiuppa et al.* [2004] carried out an inter-comparison of different methodologies (FT-IR, Filter-packs, direct sampling) on the plume; real-time measurement of volcanic H_2S and SO_2 concentrations have been measured by a UV spectroscopy prototype [*O'Dwyer et al.*, 2003]. Moreover, a comparison of H_2S fluxes from Vulcano with those of Etna and Stromboli volcanoes has been carried out to estimate the total sulphur budget at volcanoes [*Aiuppa et al.*, 2005]. Finally, *Aiuppa et al.* [2004, 2005, 2006] and *McGonigle et al.* [2008] carried out measurements to determine H_2S/SO_2 and CO_2/SO_2 ratios and relative

Table 1. Chemical Composition of High Temperature Fumaroles[a]

	FA (wt %)	F0 (wt %)
T°C	392	258
H_2O	71.02	79.16
CO_2	25.14	18.13
HF	0.02	0.02
HCl	1.07	0.91
H_2S	0.66	0.48
SO_2	0.94	0.54
He	2.5 e^{-5}	1.42 e^{-5}
H_2	1.87 e^{-3}	3.67 e^{-4}
N_2	5.9 e^{-2}	4.06 e^{-2}
CO	7.94 e^{-5}	2.04 e^{-5}
CH_4	6.46 e^{-6}	2.17 e^{-6}

[a]Average SO_2 Flux (t day^{-1}) = 12 ± 1.9.

fluxes of SO_2 with DOAS, Infra Red and electrochemical sensors.

3. CO_2 Output

[13] On the basis of previous geochemical information about hydrothermal fluids circulating inside Vulcano island and emitted into the atmosphere, we tried to estimate the total CO_2 output from the volcanic system. In particular we measured the CO_2 discharged from (1) fumaroles, (2) soil degassing, (3) bubbling gas discharges, and (4) water dissolved gases discharged from the island. For every release mode, different field data acquisition and analytical procedures have been performed. Descriptions of methodologies are given in the following sections.

3.1. La Fossa Crater Fumaroles Release

[14] The summit crater area is characterized by a wide fumarolic field with temperatures ranging from 100° to 450°C. Fumaroles show a wide range of chemical composition reflecting the level of solfataric activity with H_2O/CO_2 and CO_2/SO_2 molar ratio [*Capasso et al.*, 1997; *Paonita et al.*, 2002; *Aiuppa et al.*, 2005; *McGonigle et al.*, 2008] between 4 and 11 and 30–67, respectively. Moreover the H_2S/SO_2 molar ratio ranges from 0.4 to 2.3 [*Aiuppa et al.*, 2004, 2005].

[15] To estimate the CO_2 flux emitted from the fumaroles we chose an indirect method [*McGonigle et al.*, 2008; *Aiuppa et al.*, 2010; *Inguaggiato et al.*, 2011] based on "plume" SO_2 flux measurements and on CO_2/SO_2 ratios from fumarolic gases. The SO_2 flux measurements were carried out by a portable UV-DOAS system (MiniDOAS, see description in the next subsection). Considering the morphology of Vulcano, and on the basis of the dominant wind direction, the measurements were carried out by performing six traverse measurements from a car moving beneath the "plume." The average SO_2 flux estimated was of 12 t day^{-1} ± 1.9. This value is lower than the SO_2 fluxes measured from 1988 to 1993 (around 100 t day^{-1}) and comparable to values measured afterwards (ranging from 10 to 30 t day^{-1}) [*Barberi et al.*, 1994; *Diliberto et al.*, 2002; *Aiuppa et al.*, 2005; *McGonigle et al.*, 2008].

[16] The average values of CO_2/SO_2 ratios were determined by sampling high temperature fumaroles that were chosen on the basis of their higher volatiles fluxes of the fumarolic field (see Table 1). On the basis of the values reported in Table 1, respectively the SO_2 plume fluxes and the CO_2/SO_2 ratios of fumarolic gases, we estimated the CO_2 flux from the fumarolic area by the following relation:

$$Q_{CO2Farea} = Q_{SO2Plume} * (CO_2/SO_2)_{fumaroles}, \quad (1)$$

where $Q_{CO2Farea}$ is the flux of CO_2 evaluated for the crater plume, $Q_{SO2Plume}$ is the SO_2 flux in the plume and $(CO_2/SO_2)_{fumaroles}$ is the average weight ratio of CO_2/SO_2 in the fumaroles. The CO_2 flux resulted in about 360 t day^{-1} ± 40, for 12 t day^{-1} of SO_2 released in the plume with CO_2/SO_2 ratio of about 30.

3.1.1. Methodologies for SO_2 Flux Measurements (MiniDOAS Traverse)

[17] MiniDOAS consists of a USB2000 ultraviolet spectrometer (spectral range 245–400 nm, resolution about 0.7 nm, manufactured by Ocean Optics Inc.) and a vertically pointing telescope of 7 mrad field of view with a circular-to-linear converter 4 × 200 μm fibre bundle, which connects the telescope to the fibre. A USB cable connects the spectrometer to a laptop computer, providing power and data transfer. Software control of the USB2000 was achieved using J-scripts executed in DOASIS software (http://crusoe.iup.uniheidelberg.de/urmel/doasis/download/), to save and analyze spectra, providing real time concentration readings. Geographic coordinates for each spectrum were obtained using a handheld GPS receiver. Details of the DOAS routine used and the flux calculations can be found in the work of *Galle et al.* [2003].

3.1.2. Methodologies for Fumarole Gas Samples and Analyses

[18] In order to determine the CO_2/SO_2 ratio, two fumarolic gas samples were collected, FA and F0,

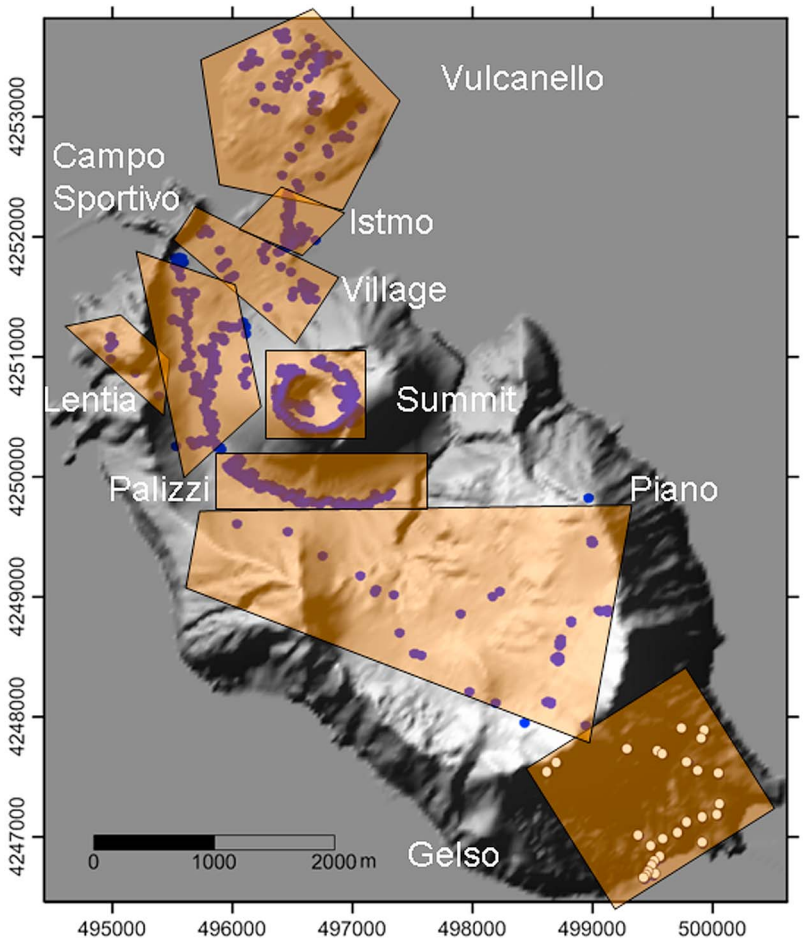

Figure 2. Location of the soil CO_2 flux measurements performed on the whole island, the exposed surface was divided into 9 areas with different measurement steps in relation to the degree of soil gas emissions.

using for each sampling site two pre-evacuated glass flasks filled with NaOH 4 M and Ammonium solution of $AgNO_3$, respectively. Within this solution steam condenses and CO_2, SO_2, HF and HCl are absorbed. These fumaroles (Figure 1) are located in the inner part (FA) of the fumarolized area and on the crater rim (F0). The whole chemical compositions of discharged gases were determined analyzing the Na-hydroxide flask. Gas phase in the head space of the flask (He, H_2, O_2, N_2, CO, CH_4) were analyzed in laboratory by using a Perkin Elmer Sigma 8500 gas chromatograph, with argon as carrier gas and equipped with Carbosieve S-II columns and HWD-FID detectors. Liquid phases (HF, HCl, S_{tot}) were determined by using liquid chromatography. Concentrations of CO_2 dissolved in alkaline solution were determined by potentiometric titration. The ratio H_2S/SO_2 was determined for the $AgNO_3$-Ammonium solution: H_2S concentration by gravimetry and SO_2 concentration by ion chromatography. The whole chemical compositions of FA and F0 fumaroles are reported in Table 1.

3.2. Soil Degassing

[19] Soil diffuse CO_2 flux output, measured according to the accumulation chamber method [*Chiodini et al.* 1998] (West Systems equipment), have been carried out on the basis of 722 measures of CO_2 fluxes in the different areas over the entire surface of Vulcano island. Figure 2 shows the location of soil flux measurement points, distributed in the respective areas of pertinence (9 areas). The density of measurement points for a single area is reported in Table 2, the measurement grid was intensified in the areas affected by major soil gas emissions as suggested by previous surveys carried out on the island [*Badalamenti et al.*, 1988, 1991; *Baubron et al.*, 1990; *Chiodini et al.*, 1996, 1998; *Diliberto et al.*, 2002]. In order to assess the

Table 2. CO_2 Flux Estimated for Single Area[a]

Study Area	Number of Samples	Area sGs (m^2)	Area (m^2)	Mean CO_2 Flux sGs (g m^{-2} day^{-1}) (Min–Max)	Standard Deviation	Total CO_2 Output From sGs (t day^{-1})	Total CO_2 Output (t day^{-1})	Min-Max (t day^{-1})
Summit	244	238,150	440,755	206 (0–1,416)	42	49	91	(0–624)
Istmo	62	40,275	40,275	122 (0–488)	65	5	5	(4–5.6)
Palizzi	76	147,700	147,700	50 (6.5–358)	16	7	7	(0.5–29)
Village	37	17,600	17,600	39 (26–207)	16	0.69	0.69	(0.36–0.97)
Campo sportivo	126	83,300	83,300	1.1 (0–2.98)	0.44	0.02	0.007	(0–0.04)
Lentia	7		13,958				0.52	(0–1.1)
Vulcanello	66	13,900	782,870	1.5 (0–9)	1	0.02	1	(0–7)
Piano	45	6,125	2,711,625	1.1 (0–1.7)	0.7	0.01	4	(0–4.6)
Gelso	29	2,800	1,202,305	0.9 (0–3.1)	0.8	0.003	1	(0–3.7)

[a]The densities of point measurements for areas are also reported.

anomaly threshold for soil CO_2 flux, normal probability plots were used (Figure 3). The entire set of measurements (722 points) corresponds to 407 data points, which on the probability plot (Figure 3) show a clear bimodal distribution, consistent with the partial overlapping of the two lognormal populations named B and H. On the basis of the technique proposed by *Sinclair* [1974], mean log flux CO_2 values of 1.24 and 2.42 g m^2 d^{-1}, standard deviations of 0.46, and relative proportion of 0.6 and 0.4, were computed for populations B and H, respectively. The mean CO_2 flux and the 95% confidence interval of the mean [*David*, 1977] are for population B 30 g m^2 d^{-1} (28–34 g m^2 d^{-1}) and for population H 455 g m^2 d^{-1} (414–512 g m^2 d^{-1}). The relatively low mean CO_2 flux for population B suggests that this population represents the background fluxes, occurring in areas that are not directly fed by uprising deep fluids (either magmatic or hydrothermal) and which could be related to the local soil biological activity. The population H is representative of the CO_2 diffuse degassing from the hydrothermal-magmatic system. Soil gas data were processed for surface mapping using the sequential Gaussian simulation (sGs), and this stochastic simulation allowed the best interpolation of the sets of data applied to evaluate the output of diffuse CO_2.

3.2.1. Summit Area

[20] The 248 measured CO_2 fluxes in randomly distributed points on the crater surface were interpolated by a distribution over a grid of 2,823 square

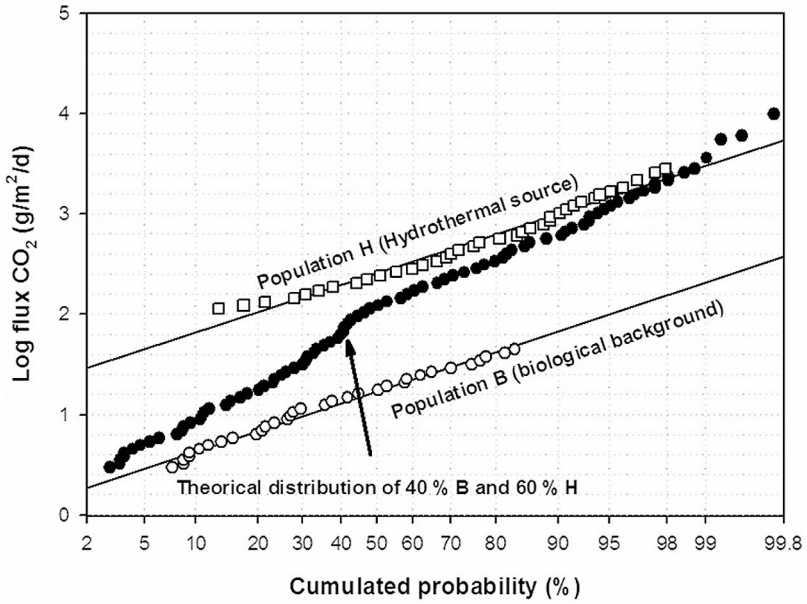

Figure 3. Normal probability plot of CO_2 fluxes. A bimodal distribution highlights the presence of two populations linked respectively to biological (B) and hydrothermal (H) sources.

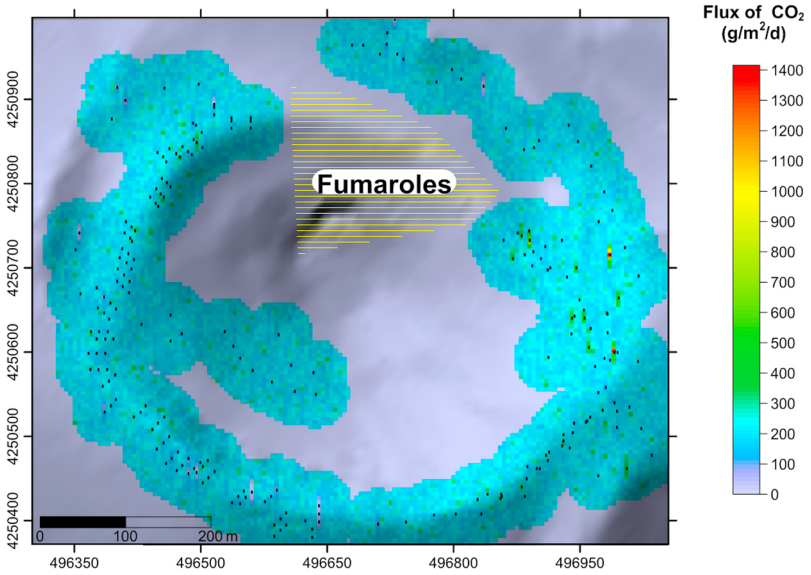

Figure 4. Map of CO_2 soil flux from the Crater area.

cells (5 × 5 m^2) covering an area of 238,150 m^2 using the so-called exponential variogram model. Then, 100 simulations of the CO_2 fluxes with the obtained distribution were performed. For each simulation, the CO_2 flux estimated at each cell is multiplied by 25 m^2 and added to the other CO_2 fluxes estimated at the other cells of the grid to have a total CO_2 output for the simulation (Figure 4). The average flux of the 100 simulations is 206 g m^2 d^{-1} with a standard deviation of 42 g m^2 d^{-1}. The mean of the 100 total simulated CO_2 outputs, 49 t day^{-1} (±), represents the estimation of the total CO_2 output from the crater area. The total area of the crater is 440,755 m^2, excluding the fumarolized area (32,755 m^2) we have a total CO_2 output of 91 t day^{-1} for an area of 408,000 m^2 (Table 2).The same kind of statistic treatment (stochastic simulation) was applied at each of the soil degassing areas and reported in Table 2 and listed below.

3.2.2. Istmo Area

[21] The 62 measured CO_2 fluxes in randomly distributed points in the Istmo area were interpolated by a distribution over a grid of 294 square cells (5 × 5 m^2) covering an area of 40,275 m^2. The mean

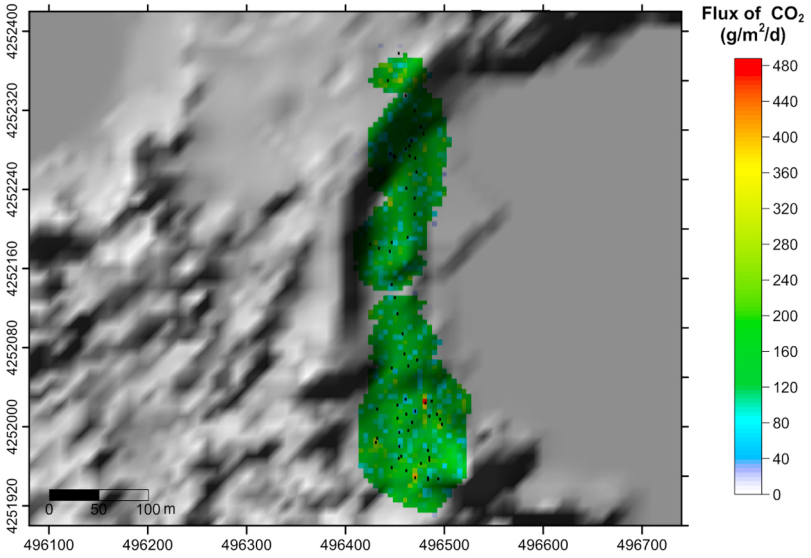

Figure 5. Map of CO_2 soil flux from the Istmo area.

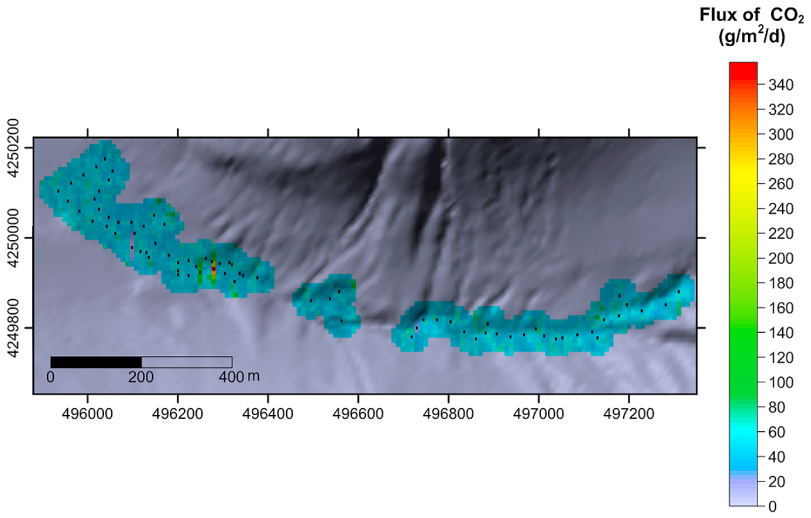

Figure 6. Map of CO_2 soil flux from the Palizzi area.

of the 100 total simulated CO_2 outputs, 5 t d^{-1}, represents the estimation of the total CO_2 output from the Istmo area with a standard deviation of 0.2 t day^{-1} (Figure 5 and Table 2).

3.2.3. Palizzi Area

[22] The 76 measured CO_2 fluxes in randomly distributed points in the Palizzi area were interpolated by a distribution over a grid of 796 square cells (10 × 10 m^2) covering an area of 147,700 m^2. The mean of the 100 total simulated CO_2 outputs, 7 t day^{-1}, represents the estimation of the total CO_2 output from the Palizzi area with a standard deviation of 0.4 t day^{-1} (Figure 6 and Table 2).

3.2.4. Village Area

[23] The 37 measured CO_2 fluxes in randomly distributed points in the village area were interpolated by a distribution over a grid of 63 square cells (5 × 5 m^2) covering an area of 17,600 m^2. The mean of the 100 total simulated CO_2 outputs, 0.67 t day^{-1}, represents the estimation of the total CO_2 output from the village area with a standard deviation of 0.01 t day^{-1} (Figure 7 and Table 2).

3.2.5. Lentia Area

[24] The very few measured CO_2 flux points in the Lentia area are not sufficient to apply the interpolation of data. In this case a simple average

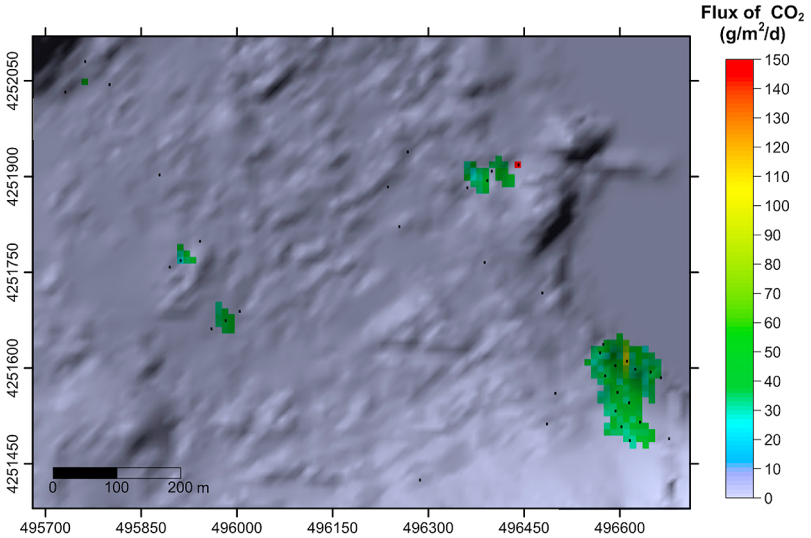

Figure 7. Map of CO_2 soil flux from the Village area.

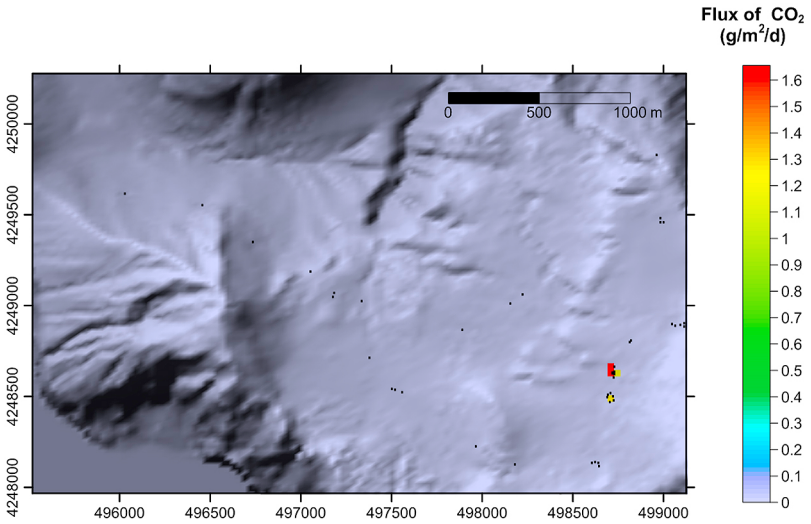

Figure 8. Map of CO_2 soil flux from the Piano area.

value calculated for the whole surface was utilized. The surface of 13,598 m^2 was considered and a total output of CO_2 of 0.5 t day^{-1} was estimated (Table 2).

3.2.6. Piano Area

[25] The 45 measured CO_2 fluxes in randomly distributed points in the Piano area were interpolated by a distribution over a grid of 5 square cells (35 × 35 m^2) covering an area of 6,125 m^2. The mean of the 100 total simulated CO_2 outputs, 4 t day^{-1}, represents the estimation of the total CO_2 output from the Piano area with a standard deviation of 0.02 t day^{-1} (Figure 8 and Table 2).

3.2.7. Gelso Area

[26] The 29 measured CO_2 fluxes in randomly distributed points in the Gelso area were interpolated by a distribution over a grid of 28 square cells (10 × 10 m^2) covering an area of 2,800 m^2. The mean of the 100 total simulated CO_2 outputs, 1 t day^{-1}, represents the estimation of the total CO_2 output from the Gelso area with a standard deviation of 0.002 t day^{-1} (Figure 9 and Table 2).

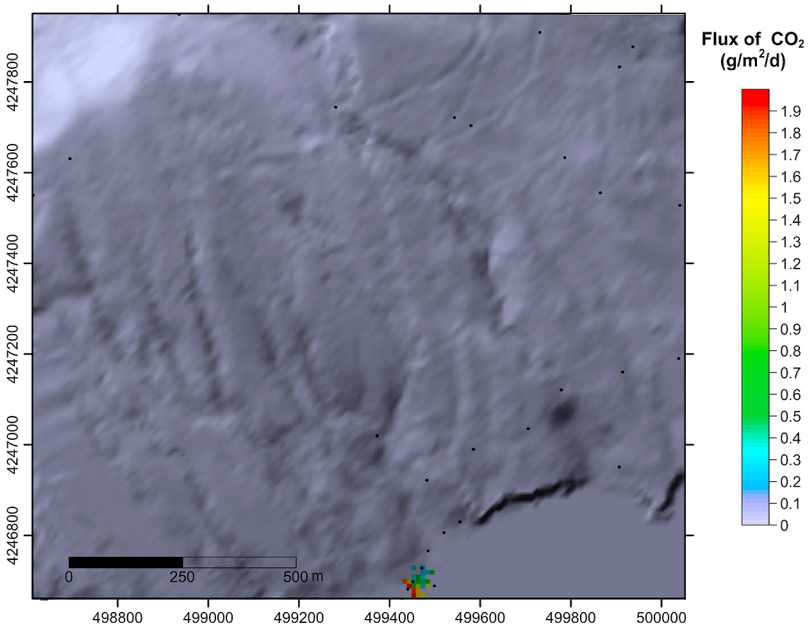

Figure 9. Map of CO_2 soil flux from the Gelso area.

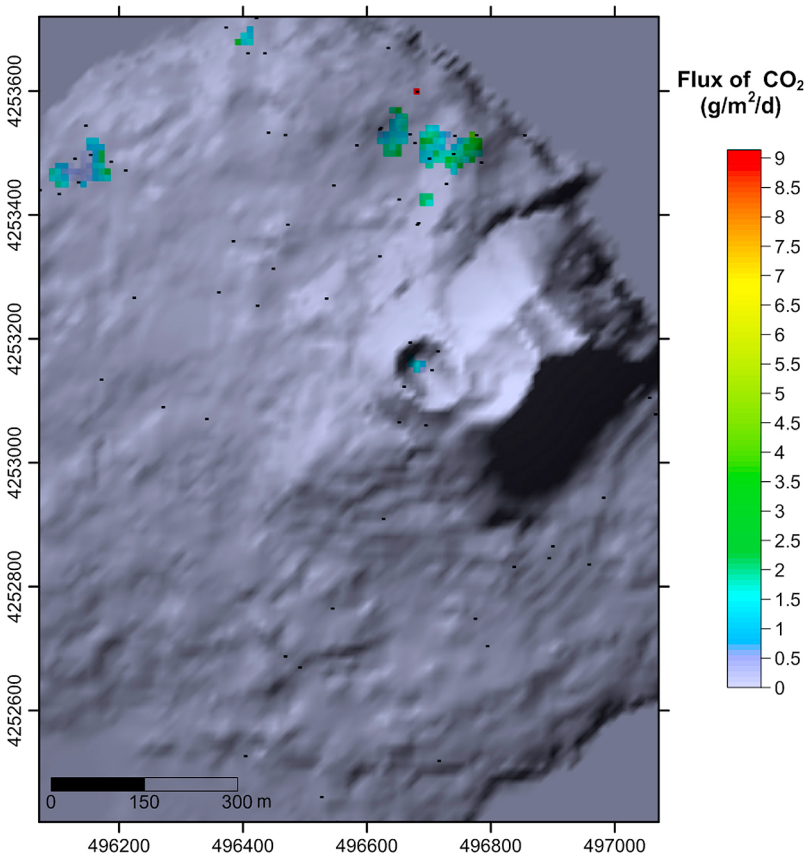

Figure 10. Map of CO_2 soil flux from the Vulcanello area.

3.2.8. Vulcanello Area

[27] The 66 measured CO_2 fluxes in randomly distributed points in the Vulcanello area were interpolated by a distribution over a grid of 139 square cells (10×10 m^2) covering an area of 13,900 m^2. The mean of the 100 total simulated CO_2 outputs, 1 t day^{-1}, represents the estimation of the total CO_2 output from the Vulcanello area with a standard deviation of 0.005 t day^{-1} (Figure 10 and Table 2).

3.2.9. Campo Sportivo Area

[28] The 126 measured CO_2 fluxes in randomly distributed points in the Campo Sportivo area were interpolated by a distribution over a grid of 208 square cells (20×20 m^2) covering an area of 83,300 m^2. The mean of the 100 total simulated CO_2 outputs, 0.02 t day^{-1}, represents the estimation of the total CO_2 output from the Vulcanello area with a standard deviation of 0.004 t day^{-1} (Figure 11 and Table 2).

[29] As a conclusive remark, the main contribution of CO_2 soil degassing to the total output is accounted by the crater soil degassing area of the active cone (91 t day^{-1}). Peripheral areas release less than 20 t day^{-1} by soil degassing (Palizzi and Istmo areas mainly) (Table 2).

3.3. Bubbling Gas Discharges

[30] To estimate the total CO_2 output flux of from bubbling gases in seawater (Istmo area) 51 point-measurements of gas flux were performed calculating the emptying-time of a 2 L plastic bottle connected to the bubbling point by an overturned funnel (Table 3). Moreover, among the 51 measurement points, five gas samples were collected to analyze the chemical composition (Table 4). The samples were collected using an overturned funnel placed just above the outlet of the degassing vent and connected to a syringe [*Gugliandolo et al.*, 1999]. Considering that the chemical composition of bubbling gases in the Istmo area is CO_2-dominated (98–99%Vol of CO_2), we estimated a total value of 3.6 t day^{-1} on the basis of the total of 51 gas fluxes measured points.

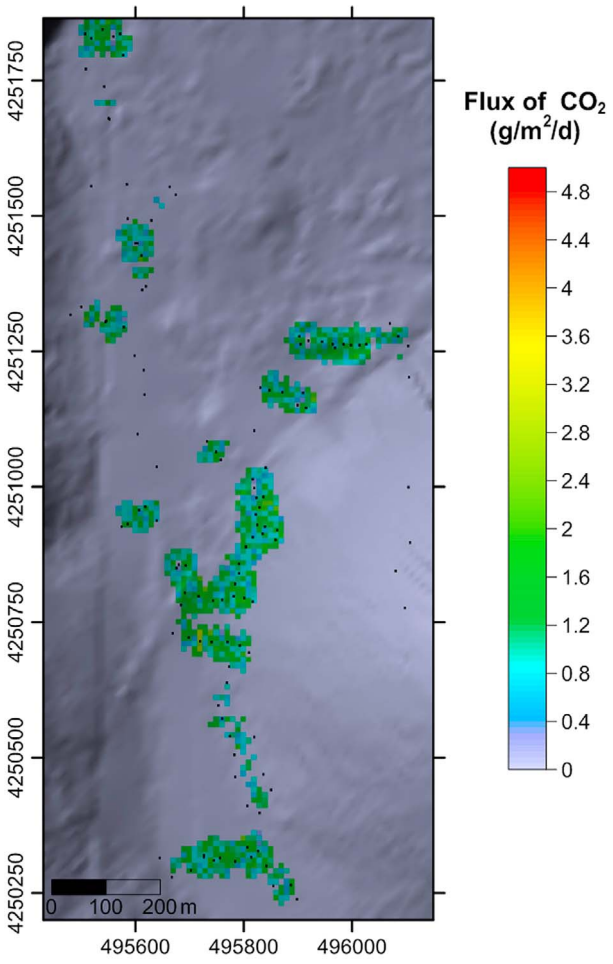

Figure 11. Map of CO_2 soil flux from the Campo Sportivo area.

3.4. Water Dissolved Gases Discharged From the Island

[31] The estimation of the dissolved gas contribution ($\phi_{CO_2}^{aquifer}$) to the total CO_2 output was carried out associating values of dissolved carbon dioxide to the aquifer discharge by the following equation:

$$\phi_{CO_2}^{aquifer} = \phi_{water}^{meteoric} \times c_{mw} + \phi_{water}^{volcanic} \times c_{vw}, \quad (2)$$

Table 3. Bubbling Gases Chemical Composition in mol%

	H_2	O_2	N_2	CH_2	CO_2
I-1	0.141	0.08	0.91	0.14	98.59
I-5	0.139	0.07	0.82	0.13	97.59
I-15	0.152	0.16	1.19	0.14	96.85
I-26	0.138	0.13	1.05	0.13	97.52
I-37	0.145	0.12	0.99	0.14	98.32

Table 4. CO_2 Flux in t day^{-1}of Bubbling Gases[a]

	liter day^{-1}	moli day^{-1}	tons day^{-1}
I-1	2,160	96	0.0042
I-2	8,640	386	0.0170
I-3	28,800	1,286	0.0566
I-4	43,200	1,929	0.0849
I-5	14,400	643	0.0283
I-6	11,520	514	0.0226
I-7	11,520	514	0.0226
I-8	11,520	514	0.0226
I-9	11,520	514	0.0226
I-10	11,520	514	0.0226
I-11	11,520	514	0.0226
I-12	43,200	1,929	0.0849
I-13	86,400	3,857	0.1697
I-14	86,400	3,857	0.1697
I-15	28,800	1,286	0.0566
I-16	14,400	643	0.0283
I-17	9,600	429	0.0189
I-18	21,600	964	0.0424
I-19	86,400	3,857	0.1697
I-20	28,800	1,286	0.0566
I-21	21,600	964	0.0424
I-22	6,646	297	0.0131
I-23	14,400	643	0.0283
I-24	28,800	1,286	0.0566
I-25	86,400	3,857	0.1697
I-26	43,200	1,929	0.0849
I-27	86,400	3,857	0.1697
I-28	28,800	1,286	0.0566
I-29	21,600	964	0.0424
I-30	86,400	3,857	0.1697
I-31	28,800	1,286	0.0566
I-32	28,800	1,286	0.0566
I-33	21,600	964	0.0424
I-34	12,343	551	0.0242
I-35	14,400	643	0.0283
I-36	43,200	1,929	0.0849
I-37	43,200	1,929	0.0849
I-38	43,200	1,929	0.0849
I-39	28,800	1,286	0.0566
I-40	43,200	1,929	0.0849
I-41	28,800	1,286	0.0566
I-42	43,200	1,929	0.0849
I-43	86,400	3,857	0.1697
I-44	86,400	3,857	0.1697
I-45	28,800	1,286	0.0566
I-46	17,280	771	0.0339
I-47	43,200	1,929	0.0849
I-48	86,400	3,857	0.1697
I-49	17,280	771	0.0339
I-50	43,200	1,929	0.0849
I-51	28,800	1,286	0.0566

[a]Total CO_2 (tons day^{-1}) = 3.61.

where c_{mw} and c_{vw} are the concentrations of the total dissolved carbonate species (CO_2 and HCO_3) in meteoric and volcanogenic components of groundwaters, respectively. Vulcano Porto aquifer is fed by two different sources: the meteoric recharge, and the condensed vapor of volcanic origin coming from the

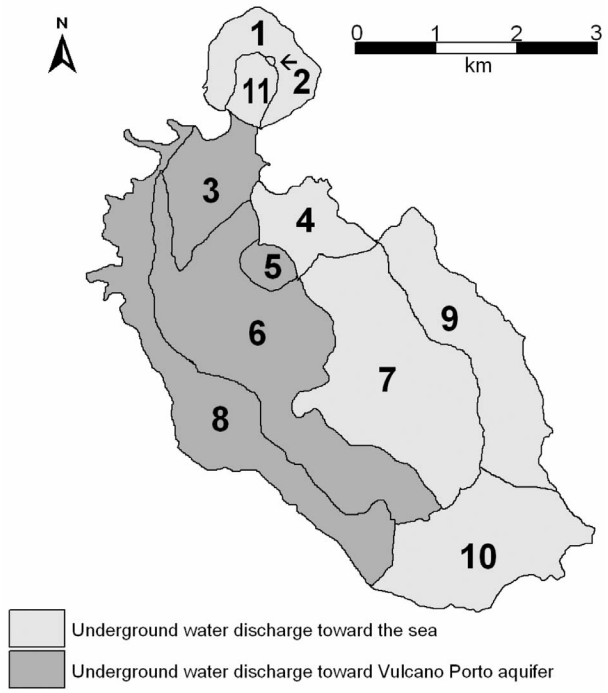

Figure 12. Classification of watersheds at Vulcano island; the recharge area of the Vulcano Porto aquifer is represented in dark gray, whereas watersheds discharging toward the sea are represented in light gray.

La Fossa crater [*Capasso et al.*, 1999]. The meteoric contribution is related both to the direct precipitation in the Vulcano Porto area and the lateral recharge coming from the other watersheds in hydro-geological connections with the coastal aquifer. The volcanic contribution consists of the lateral recharge of the coastal aquifer coming from the NW flank of the La Fossa crater, ascribable to the partial condensation of volcanogenic vapor inside the cone and its later migration toward the aquifer along volcano-stratigraphic and/or volcano-tectonic discontinuities.

[32] Clear evidence of a volcanogenic contribution to Vulcano aquifer was found by *Capasso et al.* [1999] during the volcanic crisis of 1996. They found remarkable variations in temperature, phreatic level and chemical and isotopic composition of groundwater from the Camping Sicilia well (CSI), located at the foot of the NE flank of La Fossa cone; groundwater chemical and isotopic composition indicated that during that crisis the content of fumarolic condensate in CSI well was about 80 to 90%.The estimation of the meteoric recharge was calculated by *Favara et al.* [1997] for the whole island, which is subdivided into 11 surface watersheds (see Figure 12) whose surface divides roughly correspond to the subterranean ones. Under this assumption only watersheds 3, 5, 6 and 8 feed the aquifer, whereas the meteoric discharge (both surface run-off and infiltrated rainfall) from all the others is directed toward the sea. In particular, taking into account that undergroundwaters are supposed to move along volcano-stratigraphic discontinuities, only the western sector of watershed 5, corresponding to the topographically closed depression of the La Fossa crater, contributes to the recharge of the aquifer, whereas its eastern half discharges toward the nearby watershed (4).

[33] On the basis of the hydrological balance by *Favara et al.* [1997], whose parameters are summarized in Table 5, the daily meteoric discharge of

Table 6. Total Carbon of Sampled Thermal and Cold Wells Expressed in mmoli/liter[a]

Well	T	pH	CO_2	HCO_3	Total Carbon
BAMBARA (BAM)	30.8	5.64	27.34	6.1	33.44
CASTELLO (CST)	42.3	5.54	44.54	10.2	54.74
MUSCARA' (MUS)	60.5	6.97	1.35	6.8	8.15
C.SICILIA (CSI)	52.2	7.94	0.27	5.3	5.57
LENTIA (LEN)	48.8	7.10	1.98	14	15.98
LE CALETTE (LEC)	36.8	6.78	1.54	5	6.54
DISCARICA (DIS)	48.6	6.65	16.06	41.3	57.36
EAS (EAS)	50.8	6.43	18.36	29.5	47.86
BARTOLO (BAR)	77.4	7.06	1.2	6.3	7.5
EDEN PARK (EDP)	25.8	6.84	1.1	3.6	4.7
VINCENZINO (VIN)	32.9	6.94	0.97	4.3	5.27

[a]The pH and T °C of the wells are also reported.

Table 5. Hydrological Balance for the Vulcano Porto Aquifer[a]

Watershed	3	5	6	8
Area (m^2)	1,301,778	325,587	4,659,862	3,214,150
Rainfall ($m^3\ y^{-1}$)	838,345	209,677	3,001,008	2,097,343
Evapotranspiration ($m^3\ y^{-1}$)	662,292	165,644	2,370,796	1,656,900
Average surface run-off coefficient	0.20	0.00	0.29	0.39
Average effective infiltration coefficient	0.80	1.00	0.71	0.61
Surface run-off ($m^3\ y^{-1}$)	35,096	0	180,715	172,918
Effective infiltration ($m^3\ y^{-1}$)	140,957	44,033	449,497	267,525

[a]Watershed 5 is considered as contributing 50% of it. Meteoric recharge ($m^3\ day^{-1}$) = 2,381.

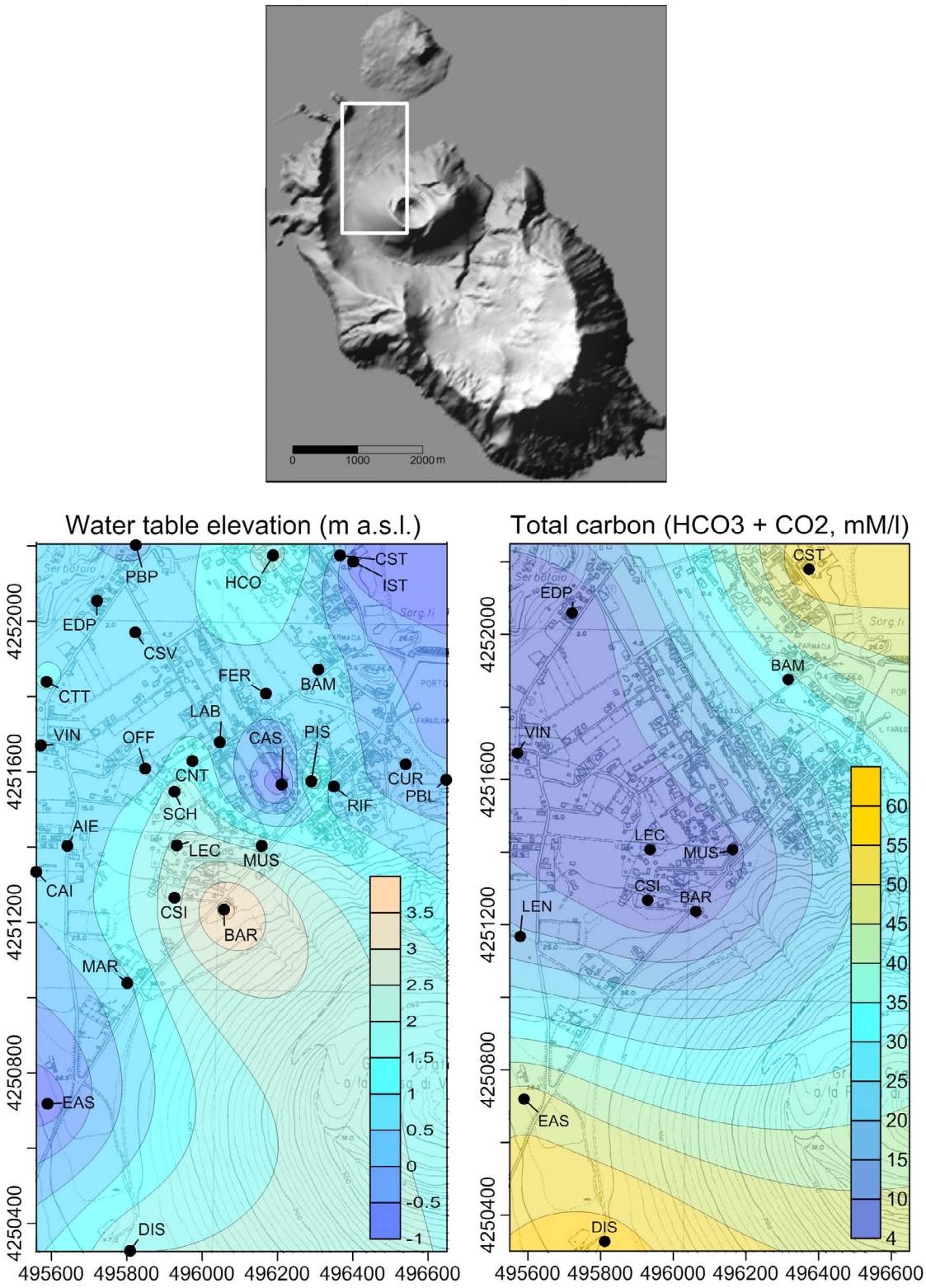

Figure 13. (bottom left) Water table elevation contour map and (bottom right) concentration of the total carbonate species in the Vulcano Porto aquifer; coordinate are expressed in UTM WGS84, 33 S Zone. (top) Altitude contour interval in the base map, extracted from the 1:10,000 Sicilian Regional Technical Cartography (CTR), is 10 m (50 m between bold lines).

Table 7. CO_2 Flux Output of Carbon Species Dissolved in the Aquifer

	H_2O Flux (t day^{-1})	Total Carbonate Concentration (mM l^{-1})	CO_2 Flux[a] (t day^{-1})
		Volcanic	
Minimum	128	6.3	0.04
Maximum	198	6.3	0.06
		Meteoric	
	2,411	43	4.56

[a]Total CO_2 flux = 4.60–4.62.

the aquifer ($\phi_{water}^{meteoric}$) has been estimated in 2,411 m^3. The volcanic recharge, due to the volcanic vapor condensed inside the La Fossa crater, may be obtained by the formula

$$\phi_{water}^{volcanic} = \phi_{CO_2}^{nf} \times X_{CO_2}^{H_2O} \times 0.5, \quad (3)$$

where V_r is the volcanic recharge in m^3/d, $\phi_{CO_2}^{nf}$ is the total flux (t day^{-1}) of carbon dioxide outside the main fumarolic field (since no significant amounts of volcanic vapor emitted from the main fumaroles condense in liquid phase due to the high temperatures), $X_{CO_2}^{H_2O}$ is the H_2O/CO_2 ratio measured in the sampled fumaroles and 0.5 is a correction coefficient inserted because, as already discussed, only the southwestern half of the crater discharges toward the aquifer. Since the daily flux of carbon dioxide outside the main fumarolic field has been evaluated in 91 t day^{-1} (see Table 2) and the water/carbon dioxide weight ratio, measured in two different fumaroles (F0 and FA), varies from 2.82 to 4.36 (see Table 1), assuming that all the water vapor emitted from the area outside the main fumarolic field condenses in the liquid phase within the volcanic edifice, the volcanic recharge ($\phi_{water}^{volcanic}$) is comprised from a minimum of 128 to a maximum of 198 t day^{-1}. The volcanic recharge, also under the maximum hypothesis, is one order of magnitude less than the meteoric contribution.

[34] The final step of the calculations consisted in associating the correct concentrations of dissolved carbon dioxide to the aquifer discharge, according to equation (2). The concentrations of the total dissolved carbonate species (CO_2 and HCO_3) of sampled waters are reported in Table 6, together with temperature and pH.

[35] In order to attribute the measured values of carbonate species to the meteoric (c_{mw}) and volcanic (c_{vw}) contributions it is necessary to correctly interpret the chemical and hydrological features of Vulcano aquifer. The water table elevation contour map presented in Figure 13 (bottom left) a clearly highlights the main features of the aquifer. The general hydraulic gradient is directed toward the sea and is cut by a piezometric high descending from La Fossa cone and passing through the wells BAR, CNT, CSI, LEC, MUS, and SCH. In our interpretation the piezometric high is due to the presence of a main regional tectonic discontinuity, known as the Tindari-Letojanni fault [*Billi et al.*, 2006], which crosses La Fossa cone. This discontinuity constitutes a preferential way for the flow of the volcanogenic groundwater component, identified by *Capasso et al.* [1999] in a single well (CSI) using isotopic and geochemical indicators, and now confirmed in CSI and other 5 wells by the piezometric features.

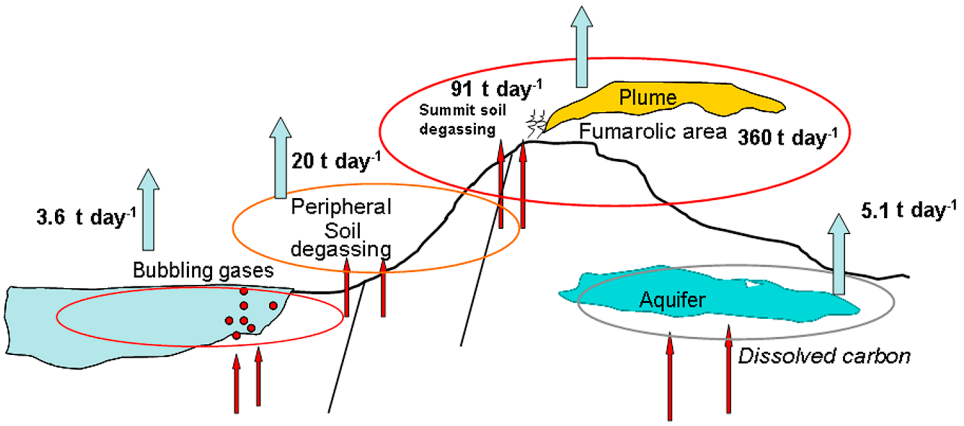

Figure 14. Total CO_2 output of Vulcano island estimated (482 t day^{-1}). The contributions of the different main areas of degassing have been reported. (a) Crater area (453 t day^{-1}), 362 and 91 t day^{-1}, respectively, for plume and summit soil degassing. (b) Total peripheral soil degassing (20 t day^{-1}). (c) Bubbling gases, main for the Istmo area (3.6 t day^{-1}). (d) Total carbon (HCO_3+ CO_2 dissolved) of aquifer (5.1 t day^{-1}).

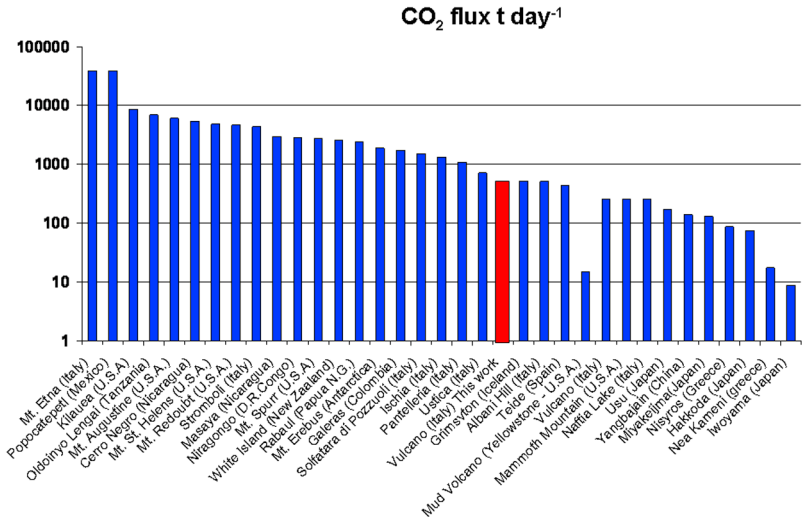

Figure 15. Total CO_2 output released from Vulcano island compared with other volcanic systems both quiescent (i.e., Pantelleria, Ischia, etc.) and at open conduct systems (i.e., Popocatépetl, Etna, etc.). Mt. Etna (Italy), 38,880 t day^{-1} [*D'Alessandro et al.*, 1997]; Popocatepetl (Mexico), 38,880 t day^{-1} [*Goff et al.*, 2001]; Kilauea (USA), 8,640 t day^{-1} [*Gerlach et al.*, 2001]; Oldoinyo Lengai (Tanzania), 6,912 t day^{-1} [*Brantley and Koepenick*, 1995]; Mt. Augustine (USA), 6,048 t day^{-1} [*Symonds et al.*, 1992]; Cerro Negro (Nicaragua), 5,443 t day^{-1} [*Salazar et al.*, 2000]; Mt. St. Helens (USA), 4,838 t day^{-1} [*Harris et al.*, 1981]; Mt. Redoubt (USA), 4,666 t day^{-1} [*Hobbs et al.*, 1991]; Stromboli (Italy), 4,320 t day^{-1} [*Allard et al.*, 1994]; Masaya (Nicaragua), 2,938 t day^{-1} [*Burton et al.*, 2000]; Niragongo (D. R. Congo) 2,851 t day^{-1} [*Le Guern*, 1987]; Mt. Spurr (USA), 2,765 t day^{-1} [*Doukas*, 1995]; White Island (New Zealand), 2,592 t day^{-1} [*Wardell et al.*, 2004]; Rabaul (Papua N. G.), 2,419 t day^{-1} [*Perez et al.*, 1998]; Mt. Erebus (Antarctica), 1,901 t day^{-1} [*Wardell et al.*, 2004]; Galeras (Colombia), 1,728 t day^{-1} [*Stix et al.*, 1997]; Solfatara di Pozzuoli (Italy), 1,512 t day^{-1} [*Cardellini et al.*, 2003]; Ischia (Italy), 1,313 t day^{-1} [*Pecoraino et al.*, 2005]; Pantelleria (Italy), 1,071 t day^{-1} [*Favara et al.*, 2001]; Ustica (Italy), 708 t day^{-1} [*Etiope et al.*, 1999]; Vulcano (Italy), 482 t day^{-1} (this study); Grimsvton (Iceland), 518 t day^{-1} [*Ágústsdóttir and Brantley*, 1994]; Albani Hill (Italy), 510 t day^{-1} [*Chiodini and Frondini*, 2001]; Teide (Spain), 432 t day^{-1} [*Mori et al.*, 2001]; Mud Volcano (Yellowstone, USA), 15 t day^{-1} [*Werner et al.*, 2000]; Vulcano (Italy), 259 t day^{-1} [*Chiodini et al.*, 1996]; Mammoth Mountain (USA), 259 t day^{-1} [*Gerlach et al.*, 2001]; Naftia Lake (Italy), 259 t day^{-1} [*De Gregorio et al.*, 2002]; Usu (Japan), 173 t day^{-1} [*Hernández et al.*, 2001a]; Yangbajain (China), 138 t day^{-1} [*Chiodini et al.*, 1998]; Miyakeijma (Japan), 130 t day^{-1} [*Hernández et al.*, 2001b]; Nisyros (Greece), 86 t day^{-1} [*Cardellini et al.*, 2003]; Hakkoda (Japan), 74 t day^{-1} [*Hernández et al.*, 2003]; Nea Kameni (Greece), 17 t day^{-1} [*Chiodini et al.*, 1998]; Iwoyama (Japan), 9 t day^{-1} [*Mori et al.*, 2001].

[36] A further element supporting this interpretation is the distribution of the dissolved carbon species (Figure 13, bottom right), which shows lower concentrations in the wells located along the piezometric high (BAR, CSI, EDP, LEC, MUS, VIN) and higher concentrations in the rest of the aquifer. Since the volcanogenic contribution in these wells is expected to be very high it is necessary to explain why carbonate species are here so depleted. In our opinion water and CO_2 are separated during the condensation process across La Fossa cone, which works as a natural equivalent of an industrial condensation column, separating different gases according to their different physico-chemical characteristics (condensation temperature, polarity and dimension of molecules, etc.); after the separation during the condensation process, water and CO_2 have very different fates: gaseous CO_2 is mainly outgassed in the atmosphere through soil and fractures, whereas liquid water depleted in carbon dioxide flows toward the coastal aquifer along volcano-sedimentary and tectono-volcanic discontinuities. On the opposite, the meteoric component of groundwater is secondary enriched in volcanic CO_2 which, driven by vertical fractures, bubbles and dissolves into the coastal aquifer. Under this assumption the simple measure of bicarbonate ions is not representative of the whole amount of CO_2 interacted with groundwater because, if a sample is taken close to a fracture from which carbon dioxide bubbles into the aquifer, a significant aliquot of this gas is still present in the dissolved phase and not as HCO_3^-; and vice versa. Thus, the sum of dissolved CO_2 and HCO_3^- concentrations has to be used for

Table 8. Computed Volatile Fluxes of Vulcano "Plume"

	t day^{-1}
H_2O	1,330
CO_2	362
HF	0.36
HCl	16.8
H_2S	9.5
SO_2	12.0
He	3.2 e^{-4}
H_2	1.6 e^{-2}
N_2	1.66
CO	7.87 e^{-4}
CH_4	6.55 e^{-5}

budgeting the total CO_2 flux from groundwater. Following these premises, the total output of CO_2 dissolved in groundwater has been calculated, using equation (2), attributing to the volcanogenic contribution the average total dissolved carbon measured in BAR, CSI, EDP, LEC, MUS, and VIN wells and to the meteoric contribution the average value measured in all the other wells; results are presented in Table 7.

4. Discussion and Conclusions

[37] A total CO_2 output of 482 t day^{-1} was estimated in September 2007 for the whole area of Vulcano island considering discharged fluids from crater fumaroles, soil degassing over the island, and bubbling and dissolved gas in the Istmo area. The main contribution to this degassing processes are the fluids discharged from the summit area of the active crater (453 t day^{-1}), with 362 and 91 t day^{-1} from crater fumaroles and crater soil degassing areas, respectively (Figure 14).

[38] The soil gas emissions from peripheral areas, respect to the active cone, was about 20 t day^{-1} CO_2, mainly from the Palizzi and Istmo areas. This value is in the same order of those for the dissolved CO_2 in thermal aquifer (5.1 t day^{-1}) and for seawater bubbling gases (3.6 t day^{-1}, Istmo area).

[39] Having measured all the different contributions to magmatic CO_2 discharged from Vulcano island, we tried to improve the comprehension of degassing system of Vulcano and to supply a value of CO_2 output to be compared with other volcanic systems in the world (Figure 15). In September 2007, Vulcano island showed a total CO_2 degassing (482 t day^{-1}) in the same order of magnitude as other quiescent volcanoes, like Teide (432 t day^{-1}), Pantelleria (1,071 t day^{-1}), and Ischia (1,313 t day^{-1}).

[40] It is very interesting to observe that the main area of discharged fluids is the summit area, with more than 90% of the total degassing, nevertheless Vulcano island is a quiescent closed conduct volcano with solphataric activity. So far, degassing processes focused on the summit area of the volcanoes have been considered typical for open conduct volcanic systems with frequent magmatic activity like Popocatépetl, Stromboli, etc. [*Inguaggiato et al.*, 2005, 2011].

[41] Fluxes of the other chemical parameters, analyzed in the discharged fumaroles, were computed in the same way as for the fumaroles CO_2 fluxes. On the basis of the measured SO_2 flux and of the total chemical composition of the analyzed fumaroles (F0 and FA) we estimated the fluxes of H_2O, HF, HCl, H_2S, CO, CH_4, and N_2. The obtained results are reported in Table 8. In particular, the flux of water vapor was estimated around 1,300 t day^{-1}. The halogens HF and HCl showed a flux of 0.36 e 16.7 t day^{-1}, respectively. H_2S fluxes (9.5 t day^{-1}) are similar to SO_2 fluxes (12 t day^{-1}). Finally, the incondensable gases, like H_2, CO, CH_4 and He, show lower fluxes, ranging from 10^{-2} to 10^{-5} t day^{-1}.

[42] On the basis of the calculated vapor released from the fumarolic area of La Fossa crater the energy release from the Vulcano island was computed. In particular, taking into account only latent heat of evaporation of water (2,500 kJ Kg^{-1}) and the estimated water flux of about 1,300 t day^{-1}, a value of energy release of about 3×10^9 kJ d^{-1} (39 MW) was estimated.

Acknowledgments

[43] The authors wish to thank their colleagues at the Istituto Nazionale di Geofisica e Vulcanologia of Palermo for their help in acquiring and processing data. They also wish to thank Franco Tassi and Takeshi Ohba for their constructive reviews that greatly improved the manuscript.

References

Ágústsdóttir, A. M., and S. L. Brantley (1994), Volatile fluxes integrated over four decades at Grimsvotn volcano, Iceland, *J. Geophys. Res.*, *99*(B5), 9505–9522, doi:10.1029/93JB03597.

Aiuppa, A., M. Burton, F. Muré, and S. Inguaggiato (2004), Intercomparison of volcanic gas monitoring methodologies performed on Vulcano Island, Italy, *Geophys. Res. Lett.*, *31*, L02610, doi:10.1029/2003GL018651.

Aiuppa, A., S. Inguaggiato, A. J. S. McGonigle, M. O'Dwyer, C. Oppenheimer, M. J. Padgett, D. Rouwet, and M. Valenza (2005), H_2S fluxes from Mt. Etna, Stromboli, and Vulcano (Italy) and implications for the sulfur budget at volcanoes,

Geochim. Cosmochim. Acta, *69*, 1861–1871, doi:10.1016/j.gca.2004.09.018.

Aiuppa, A., C. Federico, G. Giudice, S. Gurrieri, and M. Valenza (2006), Hydrothermal buffering of the SO_2/H_2S ratio in volcanic gases: Evidence from La Fossa Crater fumarolic field, Vulcano Island, *Geophys. Res. Lett.*, *33*, L21315, doi:10.1029/2006GL027730.

Aiuppa, A., et al. (2010), Patterns in the recent 2007–2008 activity of Mount Etna volcano investigated by integrated geophysical and geochemical observations, *Geochem. Geophys. Geosyst.*, *11*, Q09008, doi:10.1029/2010GC003168.

Allard, P., J. Carbonnelle, N. Métrich, H. Loyer, and P. Zettwoog (1994), Sulphur output and magma degassing budget of Stromboli volcano, *Nature*, *368*, 326–330, doi:10.1038/368326a0.

Allard, P., M. Burton, and F. Muré (2005), Spectroscopic evidence for a lava fountain driven by previously accumulated magmatic gas, *Nature*, *433*, 407–410, doi:10.1038/nature03246.

Arthur, M. A. (2000), Volcanic contributions to the carbon and sulfur geochemical cycles and global change, in *Encyclopedia of Volcanoes*, edited by H. Sigurdsson et al., pp. 1045–1056, Academic, San Diego, Calif.

Badalamenti, B., S. Gurrieri, S. Hauser, and M. Valenza (1988), Ground CO_2 output in the island of Vulcano during the period 1984–1988: Gas hazard and volcanic activity surveillance implications, *Bull. Mineral. Rend. Soc. Ital. Mineral. Petrol.*, *43*, 893–899.

Badalamenti, B., S. Gurrieri, M. Nuccio, and M. Valenza (1991), Gas hazard on Vulcano island, *Nature*, *344*, 51–53.

Barberi, F., A. Bertagnini, and P. Landi (1994), Volcanology and chemistry of earth's interior Italian research activity (1991–1994) report to IAVCEI, *Suppl. Boll. Geofis. Teor. Appl.*, *36*, supplement, 636–736.

Baubron, J. C., P. Allard, and J. P. Toutain (1990), Diffuse volcanic emissions of carbon dioxide from Volcano island, Italy, *Nature*, *344*, 51–53, doi:10.1038/344051a0.

Baubron, J. C., P. Allard, J. C. Sabroux, D. F. Tedesco, and J. P. Toutain (1991), Soil gas emanation as precursory indicators of volcanic eruptions, *J. Geol. Soc.*, *148*, 571–576, doi:10.1144/gsjgs.148.3.0571.

Billi, A., G. Barberi, C. Faccenna, G. Neri, F. Pepe, and A. Sulli (2006), Tectonics and seismicity of the Tindari Fault System, southern Italy: Crustal deformations at the transition between ongoing contractional and extensional domains located above the edge of a subducting slab, *Tectonics*, *25*, TC2006, doi:10.1029/2004TC001763.

Brantley, S., and K. Koepenick (1995), Measured carbon dioxide emissions from Oldoinyo Lengai and the skewed distribution of passive volcanic fluxes, *Geology*, *23*, 933–936, doi:10.1130/0091-7613(1995)023<0933:MCDEFO>2.3.CO;2.

Brusca, L., S. Inguaggiato, M. Longo, P. Madonia, and R. Maugeri (2004), The 2002–2003 eruption of Stromboli (Italy): Evaluation of the volcanic activity by means of continuous monitoring of soil temperature, CO_2 flux, and meteorological parameters, *Geochem. Geophys. Geosyst.*, *5*, Q12001, doi:10.1029/2004GC000732.

Burton, M. R., C. Oppenheimer, L. A. Horrocks, and P. W. Francis (2000), Remote sensing of CO_2 and H_2O emission rates from Masaya volcano, Nicaragua, *Geology*, *28*(10), 915–918, doi:10.1130/0091-7613(2000)28<915:RSOCAH>2.0.CO;2.

Capasso, G., and S. Inguaggiato (1998), A simple method for the determination of dissolved gases in natural waters. An application to thermal waters from Vulcano Island, *Appl. Geochem.*, *13*, 631–642, doi:10.1016/S0883-2927(97)00109-1.

Capasso, G., R. Favara, and S. Inguaggiato (1997), Chemical features and isotopic composition of gaseous manifestations on Vulcano Island (Aeolian Islands, Italy): An interpretative model of fluid circulation, *Geochim. Cosmochim. Acta*, *61*, 3425–3440, doi:10.1016/S0016-7037(97)00163-4.

Capasso, G., R. Favara, S. Francofonte, and S. Inguaggiato (1999), Chemical and isotopic variations in fumarolic discharge and thermal waters at Vulcano Island (Aeolian Islands, Italy) during 1996: Evidence of resumed volcanic activity), *J. Volcanol. Geotherm. Res.*, *88*, 167–175, doi:10.1016/S0377-0273(98)00111-5.

Carapezza, M. L., S. Inguaggiato, L. Brusca, and M. Longo (2004), Geochemical precursors of the activity of an open-conduit volcano: The Stromboli 2002–2003 eruptive events, *Geophys. Res. Lett.*, *31*, L07620, doi:10.1029/2004GL019614.

Carbonnelle, J., D. Dajlevic, J. Le Bronec, P. Morrel, J. C. Obert, and P. Zettwoog (1985), Etna: Composantes sommitales et parietales des emissiones de gaz carbonique, *Bull. PIRPSEV-CNRS*, *108*, 1–21.

Cardellini, C., G. Chiodini, and F. Frondini (2003), Application of stochastic simulation to CO_2 flux from soil: Mapping and quantification of gas release, *J. Geophys. Res.*, *108*(B9), 2425, doi:10.1029/2002JB002165.

Chiodini, G., and F. Frondini (2001), Carbon dioxide degassing from the Albani Hills volcanic region, Central Italy, *Chem. Geol.*, *177*(1–2), 67–83, doi:10.1016/S0009-2541(00)00382-X.

Chiodini, G., F. Frondini, and B. Raco (1996), Diffuse emission of CO_2 from the Fossa crater, Vulcano Island (Italy), *Bull. Volcanol.*, *58*, 41–50, doi:10.1007/s004450050124.

Chiodini, G., R. Cioni, M. Guidi, B. Raco, and L. Marini (1998), Soil CO_2 flux measurements in volcanic and geothermal areas, *Appl. Geochem.*, *13*, 543–552, doi:10.1016/S0883-2927(97)00076-0.

Chiodini, G., D. Granieri, R. Avino, S. Caliro, A. Costa, and C. Werner (2005), Carbon dioxide diffuse degassing and estimation of heat release from volcanic and hydrothermal systems, *J. Geophys. Res.*, *110*, B08204, doi:10.1029/2004JB003542.

D'Alessandro, W., S. Giammanco, F. Parello, and M. Valenza (1997), CO_2 output and $\delta^{13}C(CO_2)$ from Mount Etna as indicators of degassing of shallow asthenosphere, *Bull. Volcanol.*, *58*, 455–458, doi:10.1007/s004450050154.

David, M. (1977), *Geostatistical Ore Reserve Estimation*, *Dev. Geomathematics*, vol. 2, 363 pp, Elsevier, New York.

De Gregorio, S., I. S. Diliberto, S. Giammanco, S. Gurrieri, and M. Valenza (2002), Tectonic control over large-scale diffuse degassing in eastern Sicily (Italy), *Geofluids*, *2*, 273–284, doi:10.1046/j.1468-8123.2002.00043.x.

Diliberto, I. S. (2011), Long-term variations of fumarole temperature at Vulcano Island (Italy), *Ann. Geophys.*, *54*(2), 175–185, doi:10.4401/ag-5183.

Diliberto, I. S., S. Gurrieri, and M. Valenza (2002), Relationships between diffuse CO_2 emissions and volcanic activity on the island of Vulcano (Aeolian Islands, Italy) during the period 1984–1994, *Bull. Volcanol.*, *64*, 219–228, doi:10.1007/s00445-001-0198-6.

Doukas, M. P. (1995), A compilation of sulfur dioxide and carbon dioxide emission-rate data from Cook Inlet volcanoes (Redoubt, Spurr, Iliama and Augustine), Alaska, during the period from 1990 to 1994, *U.S. Geol. Surv. Open File Rep.*, *95-55*.

Etiope, G., P. Beneduce, M. Calcara, P. Favali, F. Frugoni, and M. Schiattarella (1999), Structural pattern and CO_2-CH_4

degassing of Ustica Island, S. Tyrrhenian basin, *J. Volcanol. Geotherm. Res.*, *88*, 291–304, doi:10.1016/S0377-0273(99)00010-4.

Favara, R., P. Madonia, and M. Valenza (1997), Valutazione della ricarica meteorica dell'acquifero idrotermale dell'Isola di Vulcano (Lipari, ME): Applicazione della tecnologia SIT e problematiche di modellizzazione, paper presented at Second Regional Congress of "Ordine dei Geologi di Sicilia," Ragusa, Italy.

Favara, R., S. Giammanco, S. Inguaggiato, and G. Pecoraino (2001), Preliminary estimate of CO_2 output from Pantelleria Island volcano (Sicily, Italy): Evidence of active mantle degassing, *Appl. Geochem.*, *16*, 883–894, doi:10.1016/S0883-2927(00)00055-X.

Federico, C., G. Capasso, A. Paonita, and R. Favara (2010), Effects of steam-heating processes on a stratified volcanic aquifer: Stable isotopes and dissolved gases in thermal waters of Vulcano Island (Aeolian archipelago), *J. Volcanol. Geotherm. Res.*, *192*, 178–190, doi:10.1016/j.jvolgeores.2010.02.020.

Galle, B., C. Oppenheimer, A. Geyer, A. J. S. McGonigle, M. Edmonds, and L. A. Horrocks (2003), A miniaturised ultraviolet spectrometer for remote sensing of SO_2 fluxes: A new tool for volcano surveillance, *J. Volcanol. Geotherm. Res.*, *119*, 241–254, doi:10.1016/S0377-0273(02)00356-6.

Gerlach, T. M., M. P. Doukas, K. A. McGee, and R. Kessler (2001), Soil efflux and total emission rates of magmatic CO_2 at the Horseshoe Lake tree kill, Mammoth Mountain, California, 1995–1999, *Chem. Geol.*, *177*(1–2), 101–116, doi:10.1016/S0009-2541(00)00385-5.

Goff, F., S. P. Love, R. G. Warren, D. Counce, J. Obenholzner, C. Siebe, and S. C. Schmidt (2001), Passive infrared remote sensing evidence for large, intermittent CO_2 emissions at Popocatepetl volcano, Mexico, *Chem. Geol.*, *177*, 133–156, doi:10.1016/S0009-2541(00)00387-9.

Gugliandolo, C., F. Italiano, T. L. Maugeri, S. Inguaggiato, D. Caccamo, and J. P. Amend (1999), Submarine hydrothermal vents of the Aeolian Islands: Relationship between microbial communities and thermal fluids, *Geomicrobiol. J.*, *16*, 105–117, doi:10.1080/014904599270794.

Harris, D. M., M. Sato, T. J. Casadevall, W. I. Rose, and T. J. Bornhorst (1981), Emission rates of CO_2 from plume measurements, *U.S. Geol. Surv. Prof. Pap.*, *1250*, 201–207.

Hernández, P. A., K. Notsu, J. M. Salazar, T. Mori, G. Natale, H. Okada, G. Virgili, Y. Shimoike, M. Sato, and N. M. Perez (2001a), Carbon dioxide degassing by advective flow from Usu volcano, Japan, *Science*, *292*, 83–86, doi:10.1126/science.1058450.

Hernández, P. A., J. M. Salazar, Y. Shimoike, T. Mori, K. Notsu, and N. Perez (2001b), Diffuse emission of CO_2 from Miyakejima volcano, Japan, *Chem. Geol.*, *177*(1–2), 175–185, doi:10.1016/S0009-2541(00)00390-9.

Hernández, P. A., K. Notsu, M. Tsurumi, T. Mori, M. Ohno, Y. Shimoike, J. M. L. Salazar, and N. M. Pérez (2003), Carbon dioxide emissions from soils at Hakkoda, North Japan, *J. Geophys. Res.*, *108*(B4), 2210, doi:10.1029/2002JB001847.

Hobbs, P. V., L. F. Radke, J. H. Lyons, R. J. Ferek, D. J. Coffman, and T. J. Casadevall (1991), Airborne measurements of particle and gas emissions from the 1990 volcanic eruptions of Mount Redoubt, *J. Geophys. Res.*, *96*(D10), 18,735–18,752, doi:10.1029/91JD01635.

Inguaggiato, S., G. Pecoraino, and F. D'Amore (2000), Chemical and isotopical characterization of fluid manifestations of Ischia Island (Italy), *J. Volcanol. Geotherm. Res.*, *99*, 151–178, doi:10.1016/S0377-0273(00)00158-X.

Inguaggiato, S., A. L. Martin-Del Pozzo, A. Aguayo, G. Capasso, and R. Favara (2005), Isotopic, chemical and dissolved gas constraints on spring water from Popocatépetl (Mexico): Evidence of gas-water interaction magmatic component and shallow fluids, *J. Volcanol. Geotherm. Res.*, *141*, 91–108, doi:10.1016/j.jvolgeores.2004.09.006.

Inguaggiato, S., F. Vita, D. Rouwet, N. Bobrowski, S. Morici, and A. Sollami (2011), Geochemical evidence of the renewal of volcanic activity inferred from CO_2 soil and SO_2 plume fluxes: The 2007 Stromboli eruption (Italy), *Bull. Volcanol.*, *73*, 443–456, doi:10.1007/s00445-010-0442-z.

Italiano, F., and P. M. Nuccio (1994), Gas/steam ratios and thermal energy release measured at the gaseous emission of the Baia di Levante of Vulcano Island, Italy, *Acta Vulcanol.*, *5*, 89–94.

Italiano, F., G. Pecoraino, and P. M. Nuccio (1998), Steam output from fumaroles of an active volcano: Tectonic and magmatic-hydrothermal controls on the degassing system at Vulcano (Aeolian arc), *J. Geophys. Res.*, *103*, 29,829–29,842, doi:10.1029/98JB02237.

Le Guern, F. (1987), Mechanism of energy transfer in the lava lake of Niragongo (Zaire), 1959–1977, *J. Volcanol. Geotherm. Res.*, *31*, 17–31, doi:10.1016/0377-0273(87)90003-5.

Mazot, A., D. Rouwet, Y. Taran, S. Inguaggiato, and N. Varley (2011), CO_2 and He degassing at El Chichón volcano (Chiapas, Mexico): Gas flux, origin, and relationship with local and regional tectonics, *Bull. Volcanol.*, *73*, 423–441, doi:10.1007/s00445-010-0443-y.

McGonigle, A. J. S., A. Aiuppa, G. Giudice, G. Tamburello, A. J. Hodson, and S. Gurrieri (2008), Unmanned aerial vehicle measurements of volcanic carbon dioxide fluxes, *Geophys. Res. Lett.*, *35*, L06303, doi:10.1029/2007GL032508.

Mori, T., K. Notsu, Y. Tohjima, H. Wakita, P. M. Nuccio, and F. Italiano (1995), Remote detection of fumarolic gas chemistry at Vulcano, Italy, using an FT-IR spectral radiometer, *Earth Planet. Sci. Lett.*, *134*, 219–224, doi:10.1016/0012-821X(95)00119-W.

Mori, T., P. A. Hernández, J. M. L. Salazar, N. M. Pérez, and K. Notsu (2001), An in situ method for measuring CO_2 flux from volcanic-hydrothermal fumaroles, *Chem. Geol.*, *177*(1–2), 85–99, doi:10.1016/S0009-2541(00)00384-3.

Mörner, N. A., and G. Etiope (2002), Carbon degassing from the lithosphere, *Global Planet. Change*, *33*, 185–203, doi:10.1016/S0921-8181(02)00070-X.

Nuccio, P. M., and A. Paonita (2001), Magmatic degassing of multicomponent vapors and assessment of magma depth: Application to Vulcano Island (Italy), *Earth Planet. Sci. Lett.*, *193*, 467–481, doi:10.1016/S0012-821X(01)00512-X.

O'Dwyer, M., M. J. Padgett, A. J. S. McGonigle, C. Oppenheimer, and S. Inguaggiato (2003), Real-time measurement of volcanic H_2S and SO_2 concentrations by UV spectroscopy, *Geophys. Res. Lett.*, *30*(12), 1652, doi:10.1029/2003GL017246.

Paonita, A., R. Favara, P. M. Nuccio, and F. Sortino (2002), Genesis of fumarolic emissions as inferred by isotope mass balances: CO_2 and water at Vulcano Island, Italy, *Geochim. Cosmochim. Acta*, *66*, 759–772, doi:10.1016/S0016-7037(01)00814-6.

Pecoraino, G., L. Brusca, W. D'Alessandro, S. Giammanco, S. Inguaggiato, and M. Longo (2005), Total CO_2 output from

Ischia Island volcano (Italy), *Geochem. J.*, *39*, 451–458, doi:10.2343/geochemj.39.451.

Perez, N. M., S. Nakai, K. Notsu, and B. Talai (1998), Anomalous diffuse degassing of helium-3 and CO_2 related to the active Ring-Fault structure at Rabaul Caldera, Papua New Guinea, *Eos Trans. AGU*, *79*(45), Fall Meet. Suppl., F957.

Salazar, M. L., P. A. Hernández, J. Alvarez, F. Segura, G. Melian, N. M. Perez, and K. Notzu (2000) Diffuse emission of CO_2 from Cerro Negro volcano, Nicaragua, Central America, paper presented at IAVCEI General Assembly 2000, Bali, Indonesia, 18–22 July.

Sinclair, A. J. (1974), Selection of threshold values in geochemical data using probability graphs, *J. Geochem. Explor.*, *3*, 129–149, doi:10.1016/0375-6742(74)90030-2.

Stix, J., V. M. L. Calvache, and S. N. Williams (Eds.) (1997), Galeras volcano, Colombia: Interdisciplinary study of a decade volcano, *J. Volcanol. Geotherm. Res.*, *77*, 338 pp., doi:10.1016/S0377-0273(96)00082-0.

Symonds, R. B., M. H. Reed, and W. I. Rose (1992), Origin, speciation, and fluxes of trace-element gases at Augustine volcano, Alaska: Insights into magma degassing and fumarolic processes, *Geochim. Cosmochim. Acta*, *56*, 633–657, doi:10.1016/0016-7037(92)90087-Y.

Taran, Y. A., A. D. Esikov, and A. L. Cheshko (1986), Deuterium and Oxygen-18 in waters of Mutnovsky geothermal area, *Geochem. Int.*, *4*, 458–468.

Wardell, L. J., P. R. Kyle, and C. Chaffin (2004), Carbon dioxide and carbon monoxide emission rates from an alkaline intra-plate volcano: Mt. Erebus, Antarctica, *J. Volcanol. Geotherm. Res.*, *131*, 109–121, doi:10.1016/S0377-0273(03)00320-2.

Werner, C., and C. Cardellini (2006), Comparison of carbon dioxide emissions with fluid upflow, chemistry, and geologic structures at the Rotorua geothermal system, New Zealand, *Geothermics*, *35*, 221–238, doi:10.1016/j.geothermics.2006.02.006.

Werner, C., S. L. Brantley, and K. Boomer (2000), CO_2 emissions related to the Yellowstone volcanic system: 2. Statistical sampling, total degassing, and transport mechanism, *J. Geophys. Res.*, *105*(B5), 10,831–10,846, doi:10.1029/1999JB900331.